

**SIMULATION OF OECD/NEA INTERNATIONAL STANDARD PROBLEM NO. 43 ON  
BORON MIXING TRANSIENTS IN A PRESSURIZED WATER REACTOR**

Martina Scheuerer  
Gesellschaft für Anlagen- und  
Reaktorsicherheit, Germany  
[Martina.Scheuerer@grs.de](mailto:Martina.Scheuerer@grs.de)

**ABSTRACT**

The International Standard Problem, ISP 43, was defined by the OECD/NEA and the US NRC for the validation of three-dimensional Computational Fluid Dynamics (CFD) software. The underlying experiment was performed in the 2×4 Loop Facility of the University of Maryland, College Park, U.S.A (UMCP). The test facility is a scaled-down model of the Three Mile Island TMI-2 reactor with detailed reconstruction of the reactor pressure vessel (RPV). The ISP 43 experiments focussed on rapid boron dilution transients in the RPV cold leg and downcomer. The simulations of the ISP 43 were performed with the CFX-TASCflow software. Numerical errors were monitored by comparing results obtained with different higher order discretisation schemes. Uncertainties related to physical modelling, like buoyancy effects and reactor core models, were also investigated. The simulation results show good agreement with data and prove that CFD methods can be usefully applied to this class of nuclear reactor problems.

**INTRODUCTION**

Boric acid is used as a soluble neutron absorber in the primary system of pressurized water reactors. Under normal operating conditions, the concentration of boric acid in the core is controlled by the chemical and volume control system. However, during small break loss of coolant accidents boiling and condensation can occur and de-borated water collects in the steam generator tubes and the pump suction lines, see encircled area in Fig. 1. If the de-borated water is transported into the reactor core, a heterogeneous distribution of boric acid may cause an excursion of reactivity and damage to the reactor core. Therefore, it is important to know to which extent fluid-mixing

processes can mitigate or even prevent inhomogeneous boron mixing incidents.

CFD methods are an effective tool to calculate three-dimensional mixing phenomena. Because of the rapid development of computer hardware and software, it has now become feasible to simulate transient, three-dimensional flows and the transport of de-borated water in pressurized water reactors. However, the applied numerical methods and turbulence models require experimental validation based on detailed flow and temperature fields. The ISP 43 was specifically designed and performed to provide such data for validating and assessing CFD software.

**NOMENCLATURE**

CFD	Computational fluid dynamics
CL	Cold leg
DC	Downcomer
HL	Hot leg
ISP	International standard problem
RCP	Reactor coolant pump
RPV	Reactor pressure vessel
SG	Steam generator
TMI-2	Three Mile Island, Power Plant Unit 2
UMCP	University of Maryland, College Park

**ISP 43 EXPERIMENTS**

The UMCP 2×4 Loop Facility is a scaled model of the Babcock & Wilcox TMI-2 reactor with a detailed reconstruction of the RPV. The test facility shown in Fig. 1 consists of two reactor cooling systems with two hot legs (HL), four cold legs

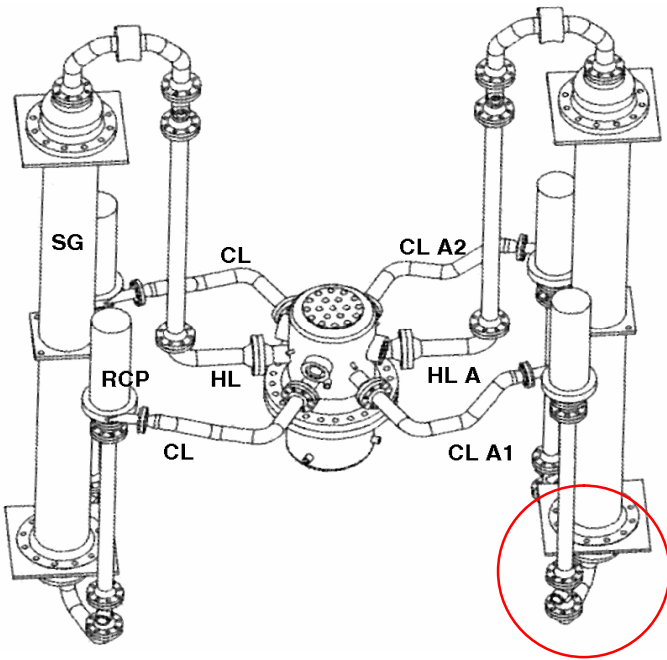


**Figure 1: UMCP 2x4 Loop Facility**

(CL) with the main coolant pumps (RCP), and two steam generators (SG). Figure 2 shows the RPV and the location of thermocouples in the downcomer (DC). The instrumentation is concentrated in the DC area to allow a detailed comparison with CFD results. Gavrilas et al. [1] give a detailed description of the test facility.

The ISP 43 consists of Test Cases A and B, see Gavrilas and Kiger [2]. In both experiments density differences between de-borated pure water and borated water are emulated by temperature differences. The reactor system is initially filled with stagnant hot water and cold water is injected into cold leg A1 by actuating the RCP. Three-dimensional mixing effects in the cold leg, and in the downcomer lead then to temporal and spatial variations of the cold water (or boron) concentration at the reactor core entrance.

In Test Case A, a continuous flow of cold water is injected into cold leg A1 from an external tank. This effectively simulates a 'water front' rather than a slug passing through the system.

In Test Case B, a finite amount of cold water is injected into the bottom of the steam generator A and the cold water slug is then set into motion by pump A.

## CFD METHOD

The calculations of the ISP 43 test cases are performed with the CFX-TASCflow software of AEA Technology, assuming transient, turbulent flow of an incompressible fluid. The mathematical model consists of the three-dimensional, ensemble-averaged conservation equations for mass, momentum and energy. The turbulent transport terms in the conservation equations of the momentum and energy equations is calculated using an

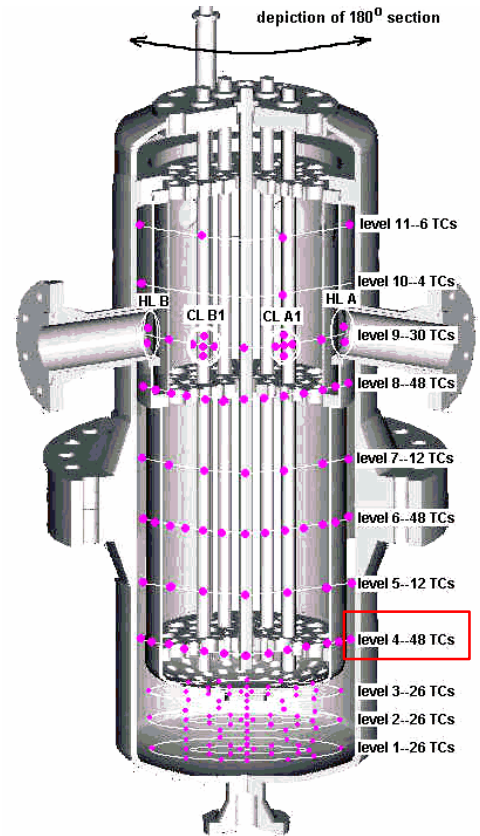


**Figure 2: Thermocouple Position**

eddy diffusivity approach in combination with the k- $\epsilon$  two-equation turbulence model see Launder and Spalding [3].

The numerical solution method of CFX-TASCflow is based on a conservative, control volume-based finite-element method with co-located variable storage. The numerical grid consists of non-orthogonal, hexahedral elements.

In the current calculations, temporally and spatially second-order accurate discretisation methods are used. The temporal discretisation method is an implicit backward Euler method using quadratic interpolation functions. The spatial discretisation schemes for the convective terms in the model differential equations are based on Raithby's [4] linear profile skew upwind methods combined with the Physical Advection Correction (PAC) method. Tri- and bi-linear form functions are used to approximate the diffusive flux terms and source or sink terms involving gradients of dependent variables with second order truncation error.

The coupled non-linear algebraic equation system arising from discretisation is linearized with a substitution or Picard scheme. CFX-TASCflow uses a pressure-based solution method, and the equations for the pressure and velocity fields are solved in a coupled manner. The resulting large coefficient matrix is solved with an iterative algebraic multi-grid method. This solution technique provides robust and rapid convergence and has a linear operation count, see [5].

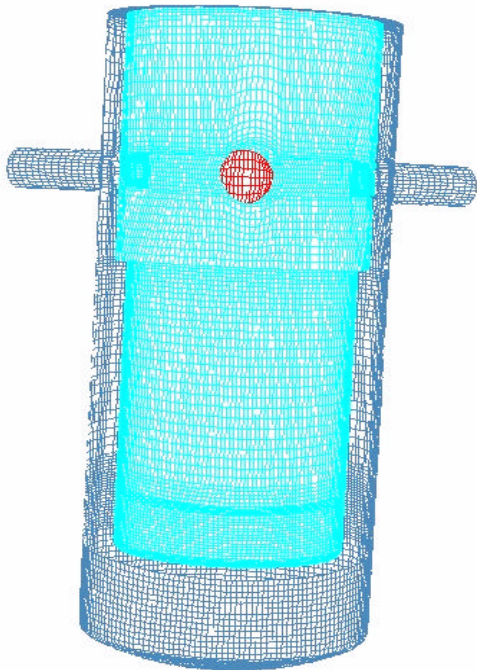


Figure 3: Numerical Grid

## COMPUTATIONS

The computational geometry is based on a three-dimensional CAD surface model in IGES format. The model is imported into the CFX-Hexa grid generation software, with which a block-structured grid with 470,000 hexahedral flux elements is generated. Figure 3 shows the surface grid of the reactor system including the cold legs, the lower plenum and the inner downcomer wall. The outlet is placed at hot leg A.

The calculations were performed on Compaq/DEC Alpha Server 8200 with 1 GB RAM. The test cases require approximately 150 h calculation time each.

### Test Case A

In Test Case A, the RPV is initially filled with warm (i.e. borated) water at a temperature of  $T = 72\text{ }^{\circ}\text{C}$ . Within 5 s the temperature of the injected water front decreases from  $72\text{ }^{\circ}\text{C}$  to  $12\text{ }^{\circ}\text{C}$ . The mass flow rate reaches its maximum value of  $7.2\text{ kg/s}$  after 27 s. Values for the velocity and length scale of the turbulence at the inlet cross section are derived from existing data. At the outlet, the average static pressure is described. The core is simulated as a porous medium with a prescribed pressure loss of 1500 Pa for steady-state conditions. The no-slip boundary condition in combination with logarithmic wall functions are applied on all inner walls of the reactor systems. The outer walls are assumed adiabatic.

As a first step in the calculation of the 'blind' Test Case A, the robustness and potential of CFX-TASCflow to predict

transient, three-dimensional, turbulent flows in the ISP 43 reactor geometry are tested using robust numerical discretisation schemes with first order accuracy. In addition, variable density and buoyancy effects are neglected. In the second step, solution errors are reduced by applying second-order accurate temporal and spatial discretisation methods. The final calculations are run with variable density and buoyancy models switched on.

The accuracy of the CFD results are assessed based on the transient circumferentially averaged temperature distribution on level 4 of the DC, see Fig. 2. Level 4 is the lowest DC level, at which temperature measurements were made. The temperature distribution at this location is an important indicator for the mixing of the de-borated cold water and the borated hot water in the RPV.

Table 1: Comparison of Average Temperatures at Level 4

$T_{\text{avg}},\text{ }^{\circ}\text{C}$	Time	24 s	28 s	32 s	36 s
<b>Experiment</b>		56.98	41.04	25.19	21.96
<b>1<sup>st</sup> Order</b>		51.82	49.64	21.95	18.17
		9.0 %	20.9 %	12.9 %	17.3 %
<b>2<sup>nd</sup> Order</b>		51.31	48.23	24.11	18.66
		9.9 %	17.5 %	4.2 %	15.0 %
<b>Buoyancy</b>		52.63	35.75	26.92	22.32
		7.6 %	12.9 %	6.9 %	1.6 %

The experimental circumferentially averaged temperatures,  $T_{\text{avg}}$ , are compared with the calculated results 24, 28, 32, and 36 s into the simulation. The third row shows the averaged temperatures calculated with first order accurate schemes. The maximum difference to the experiment is 20.9 %. The differences to the data are reduced to a maximum of 12.9 % by application of second order accurate schemes and by using variable density and buoyancy models, as shown in rows four and five of Table 1, respectively.

### Test Case B

In Test Case B, a cold-water slug is injected into the water-filled system. This experiment is closer to the reality of a deboration incident than Test Case A. Initially the coolant in the primary system is at a temperature of  $69\text{ }^{\circ}\text{C}$ . The minimum temperature of the de-borated slug is  $15\text{ }^{\circ}\text{C}$ . The transient mass flow rate and temperature distribution at the inlet of CL A1 is shown in Fig. 4. The pressure drop across the reactor core is set to 2000 Pa.

Calculations are performed with the optimised numerical and physical models of Test Case A. Figure 5 shows the temperature distribution in the DC, 20 s after start of the transient. It displays three-dimensional effects due to the non-symmetrical injection of the de-borated water plug. At the entrance of the DC, cold water flows both in the downward and in the circumferential direction. Increased temperatures appear where the DC

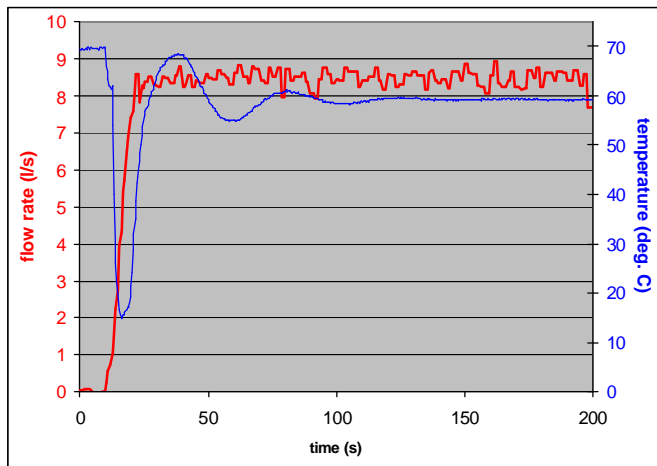


**Figure 4: Inlet Temperature and Mass Flow Rate**

width increases. These are caused by local recirculation due to the geometric discontinuity. After 20 s cold water has already reached the lower plenum where strong recirculation zones develop. The circumferential, local temperature distribution on level 4 is shown in Fig. 6. In the experiment and in the simulation the flow separates and cold water flows down on the left and right side of the inlet region. After 30 s, the injected water has almost recovered its initial temperature of 69 °C, see Fig. 7. On level 4, the temperature is still lower than at the inlet. There is strong mixing in the lower part of the vessel. The corresponding circumferential temperature on level 4 is shown in Fig. 8. The strong temperature gradients have disappeared and the fluid is well mixed. After 40 s, the DC has filled up with hot water see Fig. 9. Only in the core region, at the outlet, some colder water remains. The detailed comparison on level 4 in Fig. 10 shows good agreement between measurements and data.

## CONCLUSIONS AND OUTLOOK

The paper describes numerical simulations of boron mixing transients in a pressurised water reactor. The test cases are the ISP 43 experiments conducted at University of Maryland College Park. The simulations were performed with the CFX-TASCflow software, employing three-dimensional, averaged conservation equations for mass, momentum and energy in combination with a two-equation turbulence models.

The transient calculations described in this paper were conducted with a grid consisting of 470,000 hexahedral

elements. The results show very satisfactory agreement with measured temperatures at different measurement locations. It therefore appears that the essential three-dimensional flow structures are captured by CFX-TASCflow and that the software is well suited to studying boron injection scenarios or geometric variations of the reactor.

Future work will be concerned with quality assurance of the results, i.e. further quantification of solution errors by space and time wise grid refinement, investigation of the influence of uncertainties arising from inlet and outlet boundary conditions, from the reactor core model, and from different turbulence and near-wall models. This work will necessitate the consequential use of parallel computers to restrict and confine the required calculation times.

## ACKNOWLEDGMENTS

The author would like to acknowledge the support of the German Federal Ministry BMWi under contract INT 9113. She would also like to thank Holger Grotjans from CFX Germany for help in grid generation and Georg Scheuerer and John Stokes of CFX Germany for discussions and suggestions during the course of this work.

## REFERENCES

- [1] Gavrilas, M., Gavelli, F., Garbe, C., Parsely, E., Tafreshi, A., 1996, 'Boron-Mixing Tests in the UMCP 2x4 Loop Facility', Report UMCP-DMNE-NEP-TH001.
- [2] Gavrilas, M., Kiger, K., 2000, 'OECD/CSNI ISP Nr. 43 Rapid Boron-Dilution Transient Test for Code Verification', NEA/CSNI/R(2000)22.
- [3] Launder, B.E., Spalding, D.B., 1974, 'The Numerical Computation of Turbulent Flows', *Comp. Meth. Appl. Mech. Eng.*, Vol. 3, pp. 269 – 289.
- [4] Raithby, G. D., 1976, "Skew-Upstream Differencing Schemes for Nearly-Steady Problems Involving Fluid Flow", *Comp. Meth. Appl. Mech. Eng.*, Vol. 9, pp. 153 – 164.
- [5] Raw, M.J., 1996, 'Robustness of Coupled Algebraic Multigrid for the Navier-Stokes Equations', AIAA-Paper 96-0297.

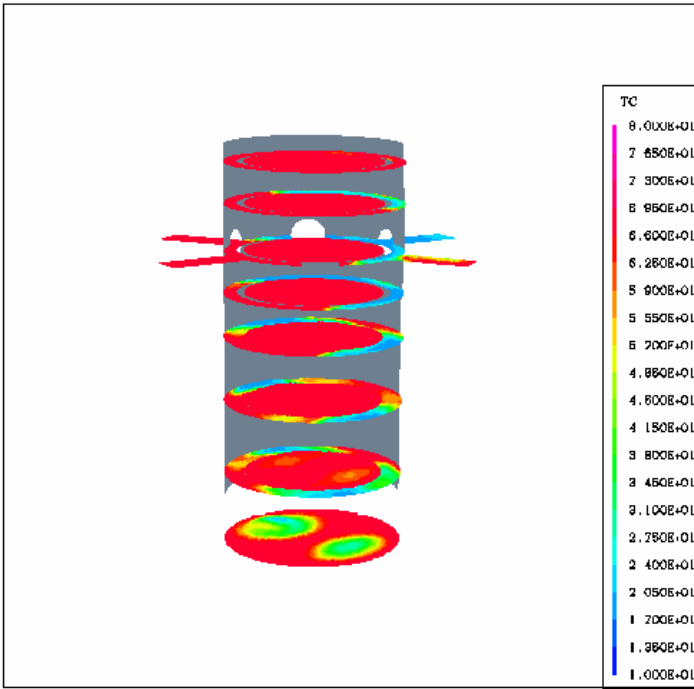


Figure 5: 3D Temperature Distribution, Time = 20 s

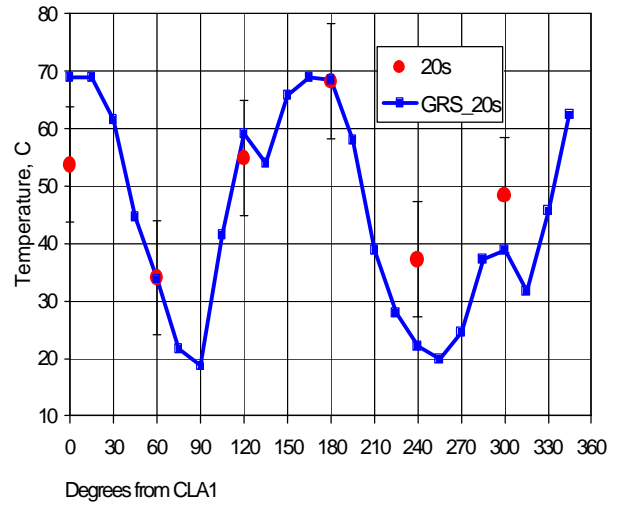


Figure 6: Local Temperature on Level 4, Time = 20 s

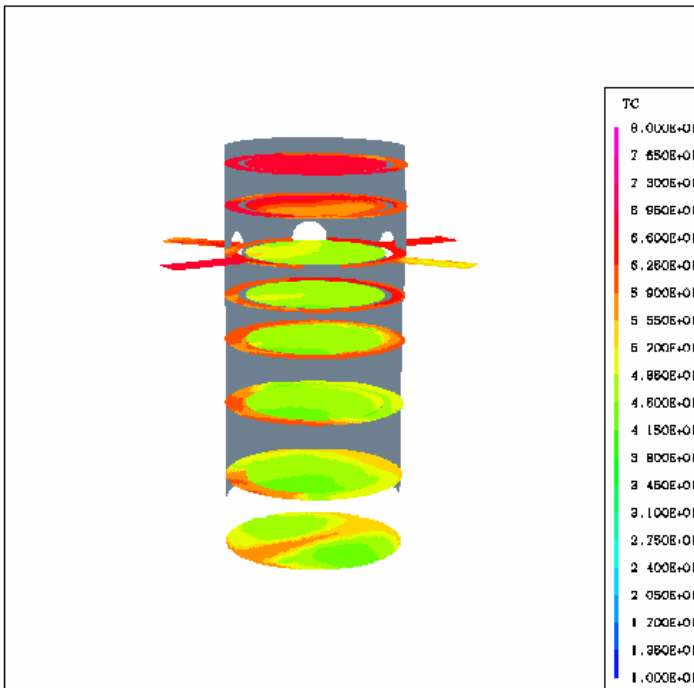


Figure 7: 3D Temperature Distribution, Time = 30 s

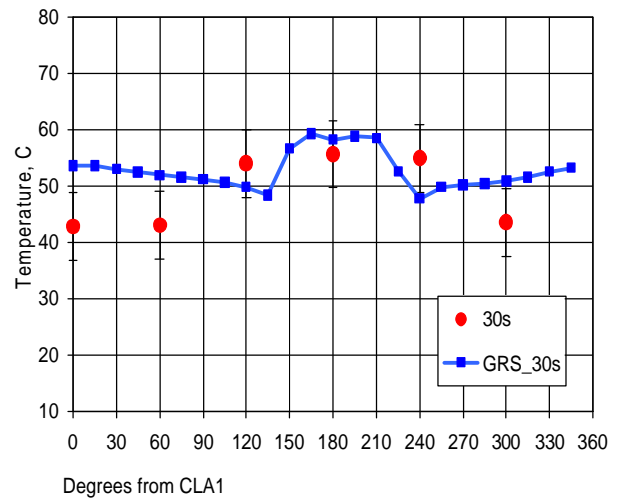


Figure 8: Local Temperature on Level 4, Time = 30 s

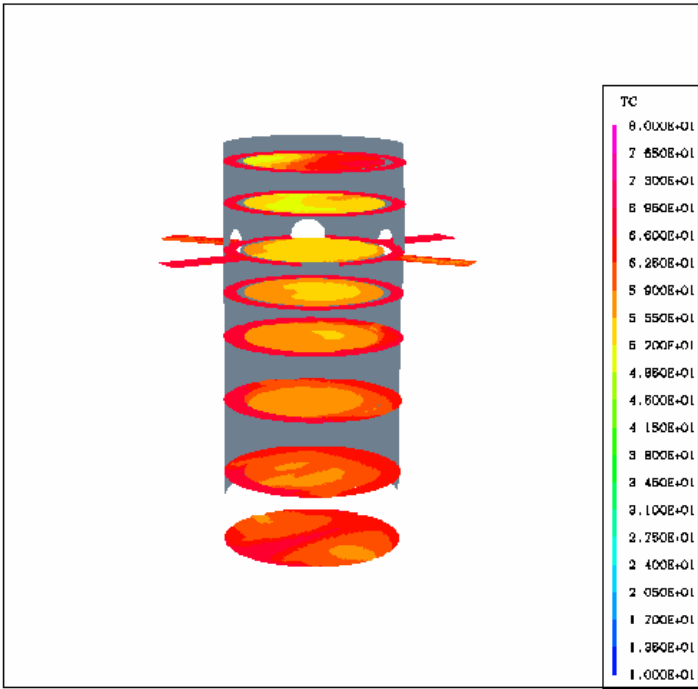


Figure 9: Temperature Distribution, Time = 40 s

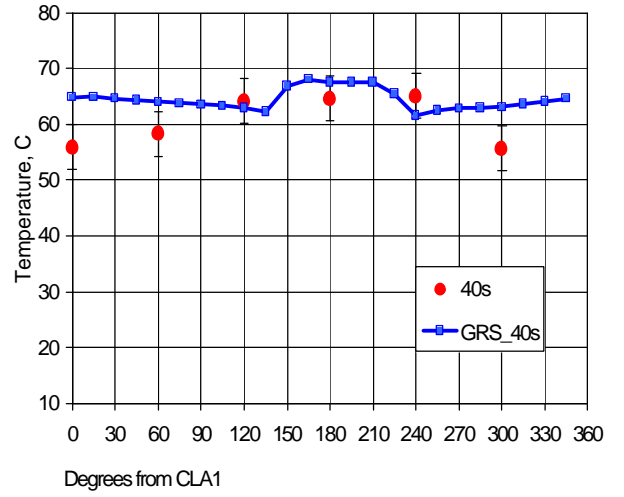


Figure 10: Local Temperature on Level 4, time = 40 s